PROCEEDINGS, Thirty-Sixth Workshop on Geothermal Reservoir Engineering
Stanford University, Stanford, California, January 31 - February 2, 2011
SGP-TR-191

RESERVOIR MODELING OF THE NORTHERN VAPOR-DOMINATED TWO-PHASE ZONE OF THE WAYANG WINDU GEOTHERMAL FIELD, JAVA, INDONESIA

Mulyadi[1] and Ali Ashat[2]

1. Star Energy Geothermal Wayang Windu Ltd., 2. Geothermal Laboratory ITB, Bandung.

mulyadi.s@starenergy.co.id

ABSTRACT

The Wayang Windu geothermal field is located 35 km southeast of Bandung, Indonesia and started commercial operation in June 2000 at 110 MWe. A second unit came on line in March 2009, to produce a total of 227 MWe. More than 90% of the steam production for the two units is supplied from a vapor-dominated two-phase zone in the north of the field.

A numerical simulation was developed to establish if this production from the two-phase zone is sustainable. The model uses TOUGH-2 simulation software. Initial and boundary conditions were defined based on available data from the drilled area. The distribution of porosity, pressure, temperature and water saturation, and their respective changes in response to exploitation were assessed. The model was verified by matching measured downhole temperatures prior to exploitation and downhole pressure and flowing enthalpies during exploitation. There is good agreement between field data and the simulation for the two-phase zone.

INTRODUCTION

The Wayang Windu geothermal field (Bogie *et al*., 2009) is located in the province of West Java, Indonesia, approximately 35 km south of the provincial capital, Bandung (Figure 1). Five high enthalpy geothermal fields occur in the Bandung area. The fields are associated with andesitic stratovolcanos of the Sunda Volcanic Arc. Besides Wayang Windu, the developed fields include Kamojang (200 MWe installed, Suryadharma *et al*, 2010) and Darajat (260 MWe installed, Suryadharma *et al*, 2010), which are both vapor-dominated geothermal systems beneath major sector collapses (Bogie *et al*., 2010). Like Wayang Windu, both Patuha (Layman and Soemarinda, 2003) and Karaha-Telaga Bodas (Moore *et al*, 2002) are liquid-dominated at depth with vapor-dominated two-phase caps and are thus transitional between vapor-dominated and liquid-dominated systems. Both fields have been drilled, but not developed.

Initial exploration of the Wayang Windu geothermal field began in 1982 when Pertamina undertook geochemical and geophysical surveys as well as drilling temperature gradient holes (Sudarman *et al*, 1986). In 1991 a deep exploration well, WWA-1 (originally designated WWD-1) was drilled (Budiardjo, 1992). This was the discovery well for the field and transitional geothermal systems; as a pre-production vapor-dominated two-phase zone was found lying above a deep liquid reservoir. Currently, a total of 39 wells have been drilled at Wayang Windu including 17 active production wells, two active reinjection wells and five slim holes. The depths of the producing wells are between 1120 m and 2510 m.

The commercial production of Unit-1 started in June 2000 with a 110 MWe single condensing turbine. A second condensing turbine was fully commissioned in March 2009 thus increasing the total installed capacity of field to 227 MWe. The two units require 450 kg/s of steam. Around 110 kg/s steam condensate is produced at 42°C and the liquid separate of around 50 kg/s with an enthalpy of 710 kJ/kg is injected into wells located in the southern part of the field. This is close to the reservoir boundary and about 2 km from the nearest production wells at the WWA pad (Figure 2).

Mass extraction (Figure 3) during early stages of operation came from both the two-phase zones and the deep liquid reservoir in the north and central parts of the field. The main production was from the two-phase zone below the MBD pad with a mixture of shallow and deep production from the MBE, WWQ and WWA pads. A strong initial decline in the pressure of the two-phase zone occurred; as would be expected for a steam-producing reservoir. However, the deep liquid feeds also showed strong production declines even after the stabilization of the two-phase zone pressures; reflecting low overall permeabilities at depth. This necessitated a make up drilling

program that targeted the northern two-phase zone from side tracks made off the less productive wells on MBD and WWQ.

The second drilling campaign for Unit-2 thus focused on the northern two-phase zone. Highly productive (averaging 40 kg/s steam) wells were drilled on the MBA, MBB, MBD and MBE pads, with the majority of production coming from the MBA pad. This resulted in approximately 90% of total steam production coming from the northern two-phase zone. A further decline in the northern two-phase zone pressure occurred with Unit 2 coming on line, but is currently in the process of stabilizing.

Further development of the field will be focused on extracting more steam from the two-phase zone in the northern part of Wayang Windu. This minimizes drilling costs, while accessing a highly permeable reservoir, with simple operation and maintenance of surface facilities.

THE NUMERICAL MODEL

Previous Models

Two numerical simulation studies have been previously made for the Wayang Windu field. The first, completed in 2002 by Unocal (the then manager of field) used the ASTRO simulator to assess the drilled area of the field and possible extensions to the north. The second numerical reservoir simulation model was developed using STARS-CMG® by MNL (now Star Energy Geothermal Wayang Windu Ltd) in 2006. The model was used to support resource assessment for the Unit-2 Wayang Windu expansion project.

Conceptual Model

Two types of thermal manifestations occur at Wayang Windu: fumaroles and steam-heated bicarbonate/sulfate hot springs. No neutral-chloride hot springs are found. The Wayang Windu reservoir consists of a lateral series of two-phase zones at shallow levels capped by a low permeability argillic layer. The argillic layer has a thickness of 800 m in the northern and 1200 m in the southern part of the field. The underlying deep liquid reservoir has temperatures > 300°C wherever it has been drilled to depth.

The reservoir rocks are andesitic volcanics, primarily tuffaceous rocks, which in the north have been intruded by microdiorite-porphyry dikes. An argillically altered zone overlies the reservoir, while propylitically altered rocks host the reservoir. The reservoir is closely associated with the young volcanic centres of Windu, Wayang, Gambung and Puncak Besar. Five different formations were defined by Bogie and MacKenzie (1997): the Wayang Windu, Malabar, Pangalengan, Waringin, and Loka. A new stratigraphic unit (the Dogdog Formation) has been recognized in the north from the results of Unit-2 drilling and is considered to be a medial andesitic stratovolcano facies of the Dogdog eruptive centre located to the east of Wayang Windu. This formation hosts the northern two-phase zone.

The Wayang Windu Geothermal field has at least three upwelling centers associated with the Windu, Wayang and Gambung volcanic centers that progressively become young to the south. Geophysical evidence suggests that a further upwelling may be associated with Puncak Besar, but this has yet to be confirmed by drilling. Two-phase zones overlying the deep liquid reservoir associated with the young volcanic centres have variable pressure, temperature and gas content. The northern two-phase zone had a pre-production temperature of 250-260°C and a pressure of 37-46 barg. The two-phase zone in the vicinity of the WWA wells was hotter at 260-270°C and possessed a correspondingly higher pressure of 50-67 barg. Temperatures in the two-phase zone at the WWF and WWW pads were 260-285 °C, and the pressure was considerably higher at 80-84 barg. The different pressure conditions reflect a higher partial pressure of non-condensable gas in the different two-phase zones from 0.5 wt% in the north, 5 wt% in the center and 20 wt% in the south.

The pressure and temperature data indicate that the various reservoirs are under-pressured with respect to ground waters requiring lateral reservoir boundaries that are essentially closed. There are no indications of lateral, deep outflows in the temperature profiles, or deep temperature reversals. Minor shallower temperature reversals and down flows in some of the deep wells have pressure profiles that indicate that they represent condensate derived from the overlying two phase zones.

The permeability encountered by the wells is mainly fracture related in the deep reservoir, but the lapilli tuffs found in the Dogdog Formation also have significant matrix permeability.

The geological, geochemical, and geophysical data have been integrated with the well results into a conceptual model of the reservoir (Figure 4). This model, which is considered a most likely description of the resource, serves as the basis for the development of a numerical simulation model. The numerical model is used to forecast the field performance under different generation scenarios in order to assess the capacity of the drilled field.

Description of Model

A 3D model numerical simulation of the Wayang Windu geothermal field has been constructed based on the existing conceptual model of the field (Figure 5). This model was developed in early 2009 using TOUGH2 simulation code (Pruess *et al*, 1999). The grid is aligned at 25^{o} east to north to align it with the longitudal axis of the field. The model covers an area of 11.25 km in the x-direction and 9.25 km in the y-direction. The top and bottom of the model were set at 2000 masl and 1200 mbsl respectively. The grid blocks have a uniform rectangular size of 187.5 m by 180 m in each layer to capture the reservoir area and well spacing. The model has 18 vertical layers in thickness from 100 m up to 200 m with finer grid blocks specified near the deep water level at 600 – 200 masl. Each layer has 3000 blocks, so there are 54,000 grid blocks, but only 16,511 active grid blocks including the blocks used to implement the base and atmospheric boundary conditions. The inactive grid blocks are dedicated for any changes of the assessed reservoir size in the future.

The model uses a distributed parameter approach. The system to be modeled becomes a number of grid block of which each interacts with another. This interaction consider variations of permeability, porosity, water saturation in reservoir and also the nature of fluid both vertically and laterally. Based on well pressure transient analysis data assessment, the model was treated to behave as a porous medium (single porosity model) and the effects of non-condensable gases were neglected. The model is set-up with connectivity between the deep liquid reservoir and the discrete two-phase zones. The rock porosity is assigned a range from 0.075 – 10 % with an average porosity of 7 % which was determined from core measurements (Asrizal *et al*, 2006). The rock density and thermal conductivity were set at 2500 – 2600 kg/m^3 and 2 – 3 W/m^2-^{o}C respectively. Permeability values assigned to the model range from 0.001 md to 250 md with maximum values in the northern two-phase zone. The specific presence of faults was not modeled. However, geological, drilling break and spinner information was used to identify permeable zones in order to assign the permeability and rock parameters of the grid blocks.

The following boundary conditions were defined to simulate the reservoir system. The base of model was setup at 1200 mbsl (layer 18). The heat source is assumed to have a constant temperature and pressure of 320^{o}C and 160 bara, which is specified beneath the reservoir zone (layer 18) with huge volume blocks. This approach has been applied previously to the Kamojang vapor-dominated reservoir (O'Sullivan *et al*, 2000). The bottom boundary is treated as impermeable, but it was assumed that there is high temperature fluid recharge into the system through several blocks at the bottom. Temperature and pressure values were adjusted until a good match with the required steam zone pressure and temperatures was obtained. Pressure and temperature at the top of the model are set at atmospheric conditions with a pressure of 1 bara and a temperature of 20^{o}C. Flows from the surface features are represented in the model by fumaroles in the north and south with a flow rate of 15 kg/s in total. The sides of the model are treated as no-flow boundaries with all sides in the model specified with zero mass and heat flows. Relative permeability was assumed to depend linearly on saturation with immobile liquid and steam saturations of 0.3 and 0.05 respectively (Corey equation). Figure 6 shows a longitudinal slice through the model. The immobile liquid saturation is assigned as 0.3 based on similar characteristic of the dry steam reservoir with Kamojang Field (O' Sullivan *et al*., 1990).

Modeling

The validation process involves matching the natural state conditions in the system and the production history, as defined by available subsurface information. The temperature distribution is compared with initial well measurements (in the undisturbed reservoir) and shut-in reservoir pressures. Enthalpy during exploitation is also compared with actual well measurement field data with the permeability structure of the model is adjusted to achieve a satisfactory match.

The natural-state model was calibrated by matching the temperature profiles of 21 wells. Eight years of production and reinjection data were used for the history match.

The Wayang Windu field is challenging and difficult to model because it contains vapor-dominated two-phase zones underlain by a liquid-dominated region. This model succeeded in producing a two-phase zone in the shallow layers of the field. Simulated results provided a good overall match to the measured downhole temperature profile of the dry steam well, MBD-4 (Figure 7) and the liquid dominated well, MBE-2 (Figure 8). Reservoir pressures and enthalpy histories of production wells with feed zone locations in the two-phase zone are in good agreement during the history matching simulation (Figure 9). However, the simulated results showed a rather poor match with the measurements in wells located in the deep liquid reservoir (Figure 10).

The forecast scenario takes 450 kg/s steam from the northern two-phase zone with make-up well targets in this area. Condensate is re-injected into the WWF-1 and WWF-3 wells at approximately 120 kg/s with enthalpy 100 kJ/kg. Liquid separate is injected to WWW-1 at approximately 60 kg/s with an enthalpy

of 710 kJ/kg. This forecast scenario is of 220 MWe when unit-2 starts online with operation up to 30 years.

DISCUSSION

Overall, the results of simulation give good agreement between model and actual field data especially in the two-phase zone layer. Fairly poor matches are indicated for wells producing (i.e. MBE-2) from the deep liquid reservoir (Figure 10). The computed reservoir pressures in these wells are too high in comparison with actual reservoir pressure field measurement. Actual deep reservoir pressure measurement has declined by 30 % rather than remaining almost constant as predicted by the model. It is possible that this disparity is caused by poor permeability and porosity data. Or that the assumed constant pressure and temperature at layer 18 utilized as the heat source is overstated.

During the exploitation, layers 5, 6, 7 of the productive steam zone layer start to dry out slowly (increasing vapor saturation) whereas the vapor saturation of the bottom steam zone layer (layer 8) decreases with time. In terms of a simple mass balance this implies that the vapour mass produced from the top layers is partly replenished by 'some' liquid mass in the lower layer. This will be beneficial since it provides some 'recharge' of the depleted steam zone layer. Currently, the effect of this phenomenon is still being assessed since few wells penetrate the deep reservoir, from which enthalpy and water level can be monitored.

The main storage of fluid and energy in the system lies in the deep brine reservoir, while the apparently easier target for steam production is represented by the shallow two-phase zone in the north. Therefore, determining the actual mass/pressure support from the underlying reservoir during exploitation of the shallow steam-dominated zone is a key issue to be carefully evaluated. Ongoing capillary tube pressure measurements are being used to monitor pressure in the deep liquid reservoir during exploitation.

CONCLUSION

The modeling of the natural state and history matching of Wayang Windu Geothermal Field has yielded results that closely match the available data and agree with the conceptual model. A forecast scenario for 220 MWe for 30 years has been met. Although the model has a reasonable match for the actual field conditions, some aspects in the model need to be improved to get better history matching of the liquid reservoir pressure, particularly regarding assumptions about deep permeabilities and recharge of the system. Further modeling is being undertaken to address this issue.

ACKNOWLEDGEMENT

The authors would like to thank the management of Star Energy Geothermal Wayang Windu for the permission to publish the paper. They also acknowledge the review of the paper by Ian Bogie.

REFERENCES

Asrizal, J. Hadi, A. Bahar and J.M. Sihombing. 2006. Uncertainty Quantification by Using Stochastic Approach in Pore Volume Calculation, Wayang Windu Geothermal Field, W. Java, Indonesia, *Proceedings*, 31th Workshop on Geothermal Reservoir Engineering, Stanford University, Stanford, CA.

Bogie, I. and Mackenzie K.M. 1998. The application of a volcanic facies model to an andesitic stratovolcano hosted geothermal system at Wayang Windu, Java, Indonesia. *Proceedings* 20th New Zealand Geothermal Workshop**.**

Bogie, I., Kusumah, Y.I., Wisnandary, C.W. 2008. Overview of the Wayang Windu Geothermal Field, West Java, Indonesia, *Geothermics*, GEOT-D-08-00009.

Bogie, I., Sugiono, S and Malik, D. 2010. Volcanic landforms that mark the successfully developed geothermal systems of Java, Indonesia identified from ASTER satellite imagery. *Proceedings* World Geothermal Congress 2010 Bali, Indonesia, 25-29 April 2010.

Budiardjo, B. 1992. Petrographic study of cores and cuttings from drillhole WWD-1. Geothermal Diploma Project Report 92.04, Engineering Library, University of Auckland, New Zealand, 43 pp.

Layman, E.B., Soemarinda, S. 2003. The Patuha vapor-dominated resource, West Java, Indonesia. In: *Proceedings* of the 28th Workshop on Geothermal Reservoir Engineering, Stanford University, Stanford, CA, USA, pp. 56-65.

Pruess, K., Oldenburg, C., Moridis, G. 1999. TOUGH2 User's Guide Version 2.0, Ernest University of California, Lawrence Berkeley National Laboratory, Earth Sciences Division.

Moore, J.N., Allis, R., Renner, J.L., Mildenhall, D., McCulloch, J. 2002. Petrological evidence for boiling to dryness in the Karaha-Telega Bodas geothermal system, Indonesia. *Proceedings* of the 27th Workshop

on Geothermal Reservoir Engineering, Stanford University, Stanford, CA, USA, pp. 223-232.

O'Sullivan, M., Pruess, Karsten., Lippmann, Marcelo. 2000. Geothermal Reservoir Simulation: The State-of-practice and Emerging Trends, World Geothermal Congress, Kyushu-Tohoku, Japan.

O'Sullivan, M.J., Barnett, B.G., and Razali, M.Y. 1990. Numerical Simulation of the Kamojang Geothermal Field, Indonesia, Geothermal Resources Council Transactions, Vol. 14, Part II.

Sudarman, S., Pujianto, R., Budiarjo, B. 1986. The Gunung Wayang Windu geothermal area in West Java. *Proceedings* of the 15th Annual Convention of the Indonesian Petroleum Association, pp. 141-153.

Suryadarma, et al. 2010. Geothermal Energy Update: Geothermal Energy Development and Utilization in Indonesia. *Proceedings* of the World Geothermal Congress.

FIGURES

Figure 1: Wayang Windu located in cluster of high enthalpy geothermal fields.

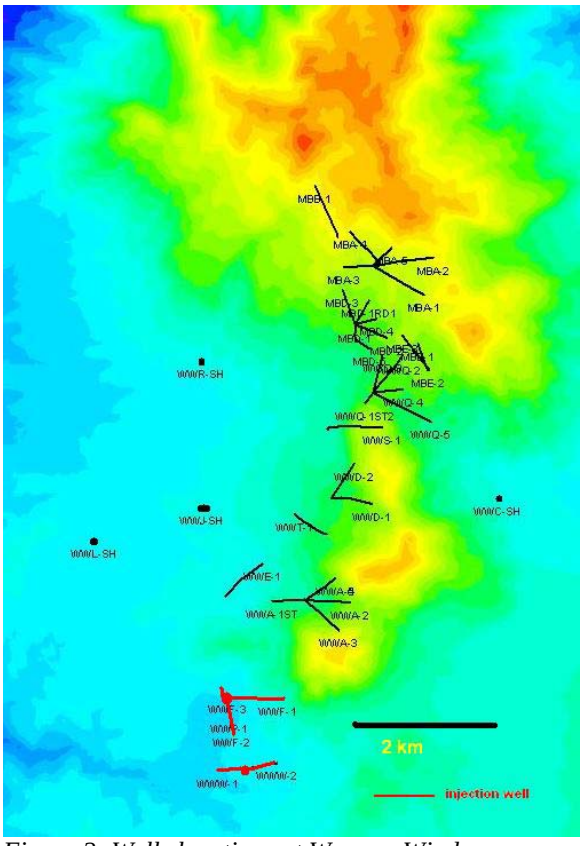

Figure 2: Wells locations at Wayang Windu.

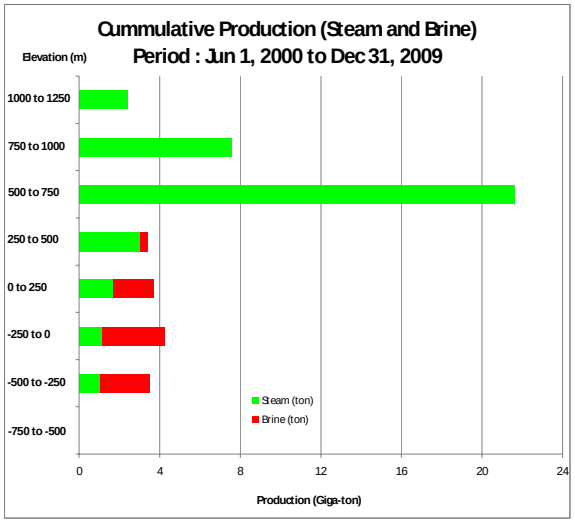

Figure 3: Cumulative production history versus depth.

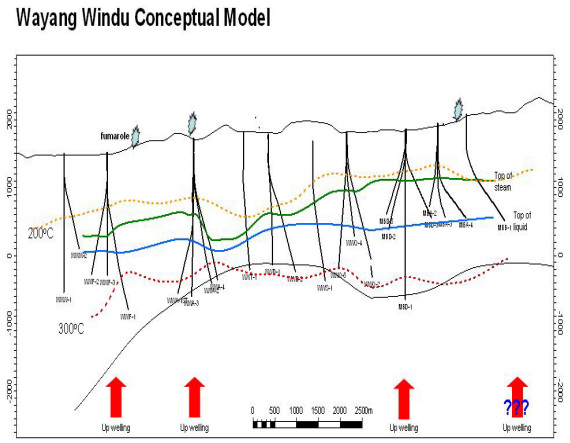

Figure 4: Wayang Windu conceptual model description.

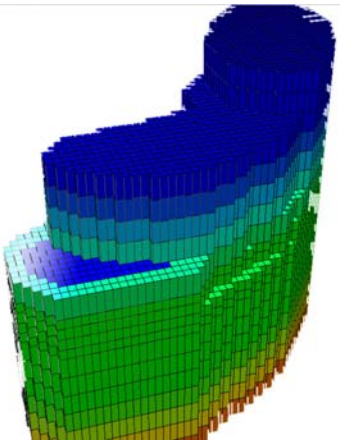

Figure 5: Longitudinal cross section through the Wayang Windu field.

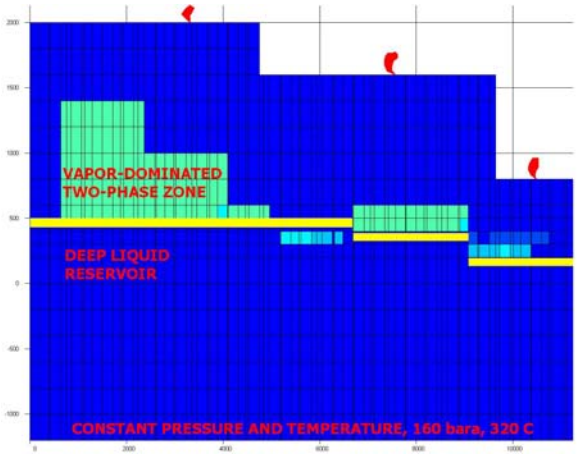

Figure 6: Description of Wayang Windu model

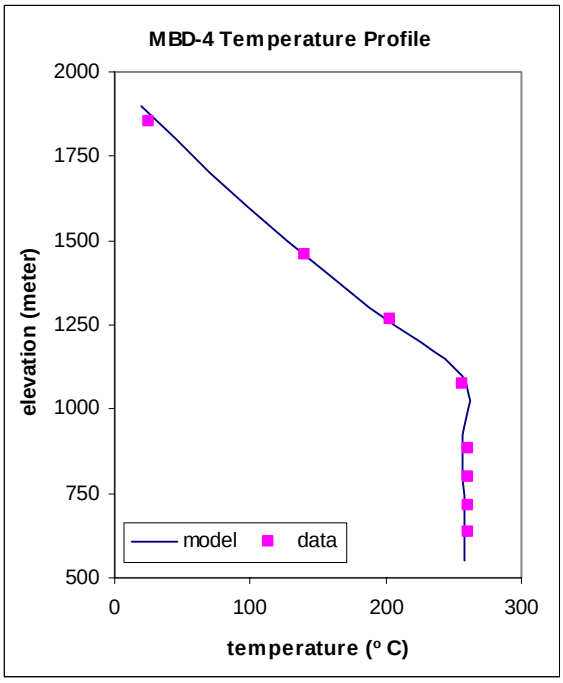

Figure 7: MBD-4 temperature matching in natural state condition

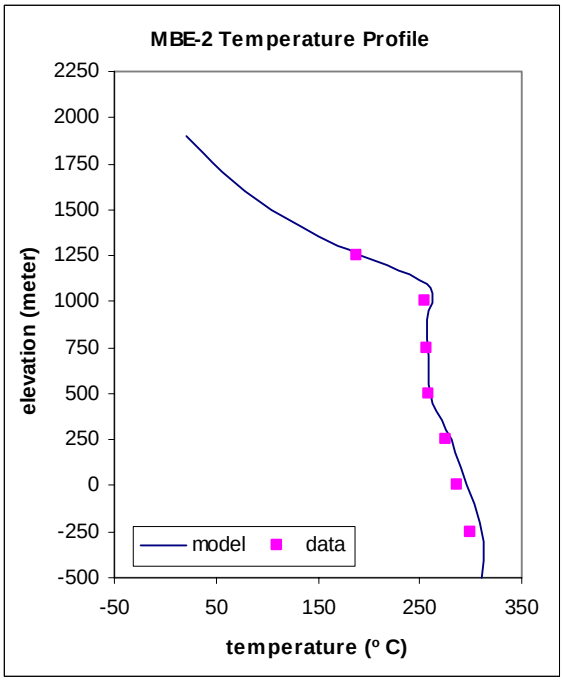

Figure 8: MBE-2 temperature matching in natural state condition

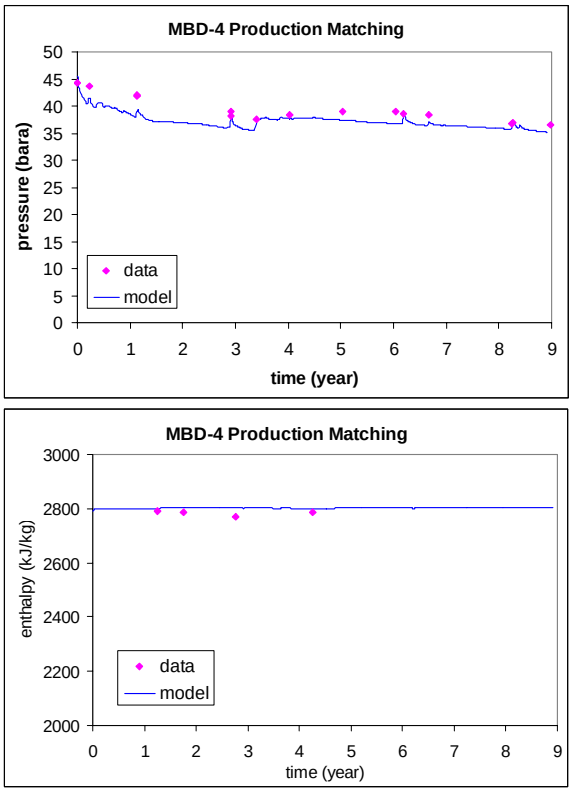

Figure 9: MBD-4 pressure and enthalpy matching during exploitation

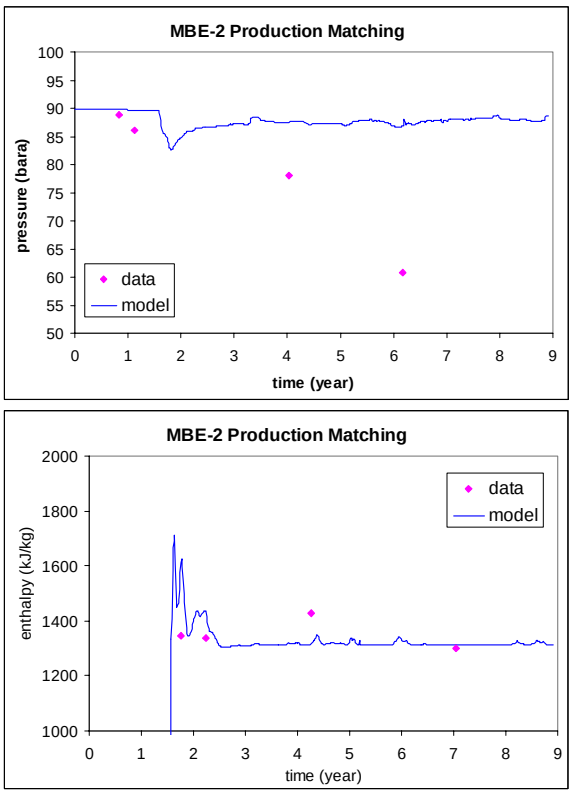

Figure 10: MBE-2 pressure and enthalpy matching during exploitation